

# Study of soil gas radon variations in the tectonically active Dharamshala and Chamba regions, Himachal Pradesh, India

Arvind Kumar · Vishal Arora · Vivek Walia ·  
Bikramjit Singh Bajwa · Surinder Singh ·  
Tsanyao Frank Yang

Received: 28 December 2012 / Accepted: 27 February 2014 / Published online: 17 March 2014  
© Springer-Verlag Berlin Heidelberg 2014

**Abstract** Soil gas radon measurements were made in Chamba and Dharamshala regions of Himachal Pradesh, India, to study the correlation, if any, between the soil gas radon, radium activity concentration of soil, and the geology/active tectonics of the study region. Soil gas radon surveys were conducted around the local fault zones to check their tectonic activities using the soil gas technique. Soil gas radon activity concentration at thirty-five different locations in Dharamshala region has been found to be varying from  $13.2 \pm 1.5$  to  $110.8 \pm 5.0$  kBq m<sup>-3</sup> with a geometrical mean of  $35.9$  kBq m<sup>-3</sup> and geometrical standard deviation of 1.8. Radon activity concentration observed in the thirty-seven soil gas samples collected from the Chamba region of Himachal Pradesh varies from  $5.2 \pm 1.0$  to  $35.6 \pm 2.5$  kBq m<sup>-3</sup>, with geometrical mean of  $15.8$  kBq m<sup>-3</sup> and geometrical standard deviation of 1.6. Average radium activity concentrations in thirty-four soil samples collected from different geological formations of Dharamshala region and Chamba region are found to be  $40.4 \pm 17$  and  $38.6 \pm 1.7$  Bq kg<sup>-1</sup>, respectively. It has been observed that soil gas radon activity concentration has a wide range of variation in both Dharamshala and Chamba regions, while radium activity concentrations in soil

samples are more or less same in both the regions. Moreover, soil gas radon activity concentration has a better positive correlation with the radium activity concentration in soil samples collected from Chamba region as compared to Dharamshala region.

**Keywords** Soil gas · Radon · Radium · Faults · NW Himalayas

## Introduction

Migration of radon in soils occurs by different processes viz. diffusion, advective, and convective flows (Fu et al. 2005; Tanner 1964). Radon appears mainly by diffusion process from the point of origin following  $\alpha$ -decay of <sup>226</sup>Ra in underground soil. Radon can originate from deeply buried deposits and can migrate to the soil surface. Various studies have shown that a strong relation exists between geology and radon in soil gas (Bolinder et al. 1993; Choubey et al. 1999, 2000, 2001, 2005; Gundersen et al. 1988; Schumann and Owen 1988). Recent advances in the application of soil gas survey have shown the potential of radon measurements for studying both fault activity and seismic hazards for a region (Ciotoli et al. 2007, 1998; Fu et al. 2005; Kumar et al. 2009, 2012, 2013; Walia et al. 2006, 2009a, b, 2013). The high concentrations characteristic of radon over faults reflect gas migration dominated by brittle deformation both at macro- and/or microscale. Therefore, spatial patterns of soil gas radon in faulted areas appear to be suitable tools for identifying and mapping active tectonic structures (Baubron et al. 2002; Ciotoli et al. 1998, 1999; Crenshaw et al. 1982; Cox 1983; Papastefanou et al. 2001; Williams 1985). Faults and fractures in the underlying rocks provide paths of high

A. Kumar · V. Walia (✉)  
National Centre for Research on Earthquake Engineering,  
NARL, Taipei 106, Taiwan  
e-mail: vivekwalia@rediffmail.com; walia@ncree.org.tw

V. Arora · B. S. Bajwa · S. Singh  
Department of Physics, Guru Nanak Dev University,  
Amritsar 143005, India

T. F. Yang  
Department of Geosciences, National Taiwan University,  
Taipei 106, Taiwan

permeability and therefore serve as conduits for radon gas migration. High concentrations of soil gases are more prominent along fault lines and at their intersections (Etiopo and Lombardi 1995; King et al. 1996). On the contrary, presence of fault near the sampling locations does not always produce anomalous radon activity concentration as the behavior of soil gas radon is also controlled by other factors in the study region. In recent studies in the vicinity of Ravne fault in NW Slovenia, the concentrations of radon in soil gas were found to be lower than the average for Slovenia and anomalous radon activity concentrations were not observed near the fault (Vaupotic et al. 2010).

In the present investigations, the soil gas radon measurements were carried out in tectonically active regions of Chamba and Dharamshala in the NW Himalayas, India, using RAD7 detector. Radon activity concentrations in soil gas were measured at various distances from the tectonic structures in the study region, in order to find their influence on radon transport. The samples were collected from different geological formations along and across the various regional fault zones. The aim of the present work was to study the correlation, if any, between the soil gas radon, radium activity concentration of soil, and the geology/active tectonics of the study region.

## Geology of area

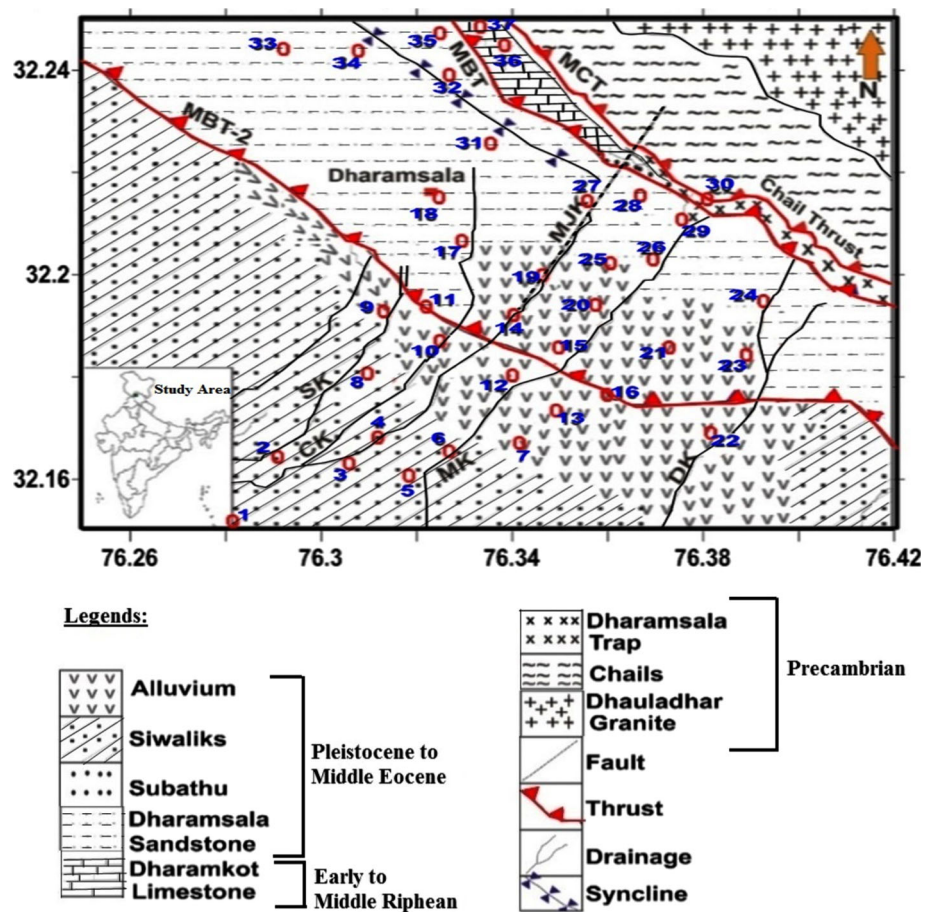
Himalayan region is being subjected to intense neotectonic movements and seismic activities (Joshi 2004; Kothiyari et al. 2010; Thakur 1998). For systematic study, the study area has been divided into two regions viz. Dharamshala region and Chamba region on the basis of lithology and thrust systems of the area.

Dharamshala region (Fig. 1) of the NW Himalayas lies on the southern slope of the Dhauladhar range. Diverse lithology within a short span of distance makes the study area tectonically significant and shows the features of ductile shear zone due to the presence of distinct thrust planes popularly known as Main Boundary Thrust (MBT-2, locally known as Drini Thrust), MBT, and Main Central Thrust (MCT, locally known as Chail Thrust) (Mahajan et al. 1997). In this region, the individual formations and groups are separated from one another by longitudinal thrust systems (Mahajan and Viridi 2000), and the area is crosscut by transverse faults/lineaments trending NE–SW. Dharamshala group has been named after Dharamshala town and consists of fine to medium grained dirty gray to maroon compact, jointed, and non-micaceous sandstones which are interbedded with clay bands of crimson red, green, and maroon color. It is generally believed that provenance for the rocks of Shiwalik formation are the

metamorphic and sedimentary rocks, and these rocks consist essentially of a thick succession of sandstone, shale, clays, and conglomerates in parts of lower Dharamshala. Dharamkot formation is named after the Dharamkot village and extends from Kareri in the NW to the Khaniyara in the east of Dharamshala. It is believed that these traps were poured out at the time of epiorogenic movements which were of widespread scale and nearly affected the entire belt of Himalayas and have been characterized by the presence of basic volcanic rocks with structure characteristics of lavas and tuffs in Dharamshala traps. The limestone succession of Dharamkot formation and Dharamshala traps is sandwiched between two steeply inclined thrusts. Dharamshala is located very close to the perennial snowline and surrounded by deodar forests and the Dhauladhar range, the mighty snowy mountains of Dharamshala. These mountains rise about 4,000 m above the floor of the valley. Dharamshala has an average elevation of 1,457 m (4,780 feet). Chamba region (Fig. 2) forms a part of the wide longitudinal valley that lies between the Zaskar and Dhauladhar ranges in the north and south, respectively. The valley trends NW–SE and is considered to be of tectonic origin (Gansser 1964; Wadia 1957). The southern part of the longitudinal valley is known as the Chamba valley, and the northwestern part is known as Kashmir valley. Various tectonic features in Chamba region are Muree thrust (MT), Suloh thrust (ST), MBT, and Panjal thrust (PT) (Fig. 1). The area is seismically active and lies in the high-risk seismic zone of India. Lower part of Chamba formation consists of monotonous alternations of metagraywacke and slate-forming sandy flysh. Upper part of this formation comprises of alterations of slate and metasiltstone metagraywacke, showing turbidite structures in shally flysh sequence. Salkhala formation in the Chamba region consists of phyllite, quartzitic phyllite, micaceous quartzites, and occasional bands of gray marbles and volcanic layers together with biotite and garnet-biotite schists near the granitic bodies. Chamba district presents an intricate mosaic of mountain ranges, hills, and valleys. It is primarily a hilly district with altitudes ranging from 600 to 6,400 m amsl. Physiographically, the area forms a part of the middle Himalayas with high peaks ranging in height from 3,000 to 6,000 m amsl. It is a region of complex folding, which has undergone many orogeneses. The topography of the area is rugged with high mountains and deep dissected by river Ravi and its tributaries. Physiographically, the district can be divided into two units viz. (1) high hills, which cover almost entire district, and (2) few valley fills.

In the present study, sampling is done longitudinally along the MT, ST, MBT, and PT in the Chamba (Fig. 2), while in Dharamshala region, sampling is done across the MBT-2, MBT, MCT, and along the various transverse lineaments running parallel to drainage systems (Fig. 1).

**Fig. 1** Geological map of Dharamshala region along with the measurement points and tectonic features (MBT = Main Boundary Thrust, MCT = Main Central Thrust) and drainage systems (SK = Sarah Khad, CK = Churan Khad, MJK = Manjhi Khad, MK = Manuni Khad, DK = Darun Khad) (modified after Walia et al. 2008)

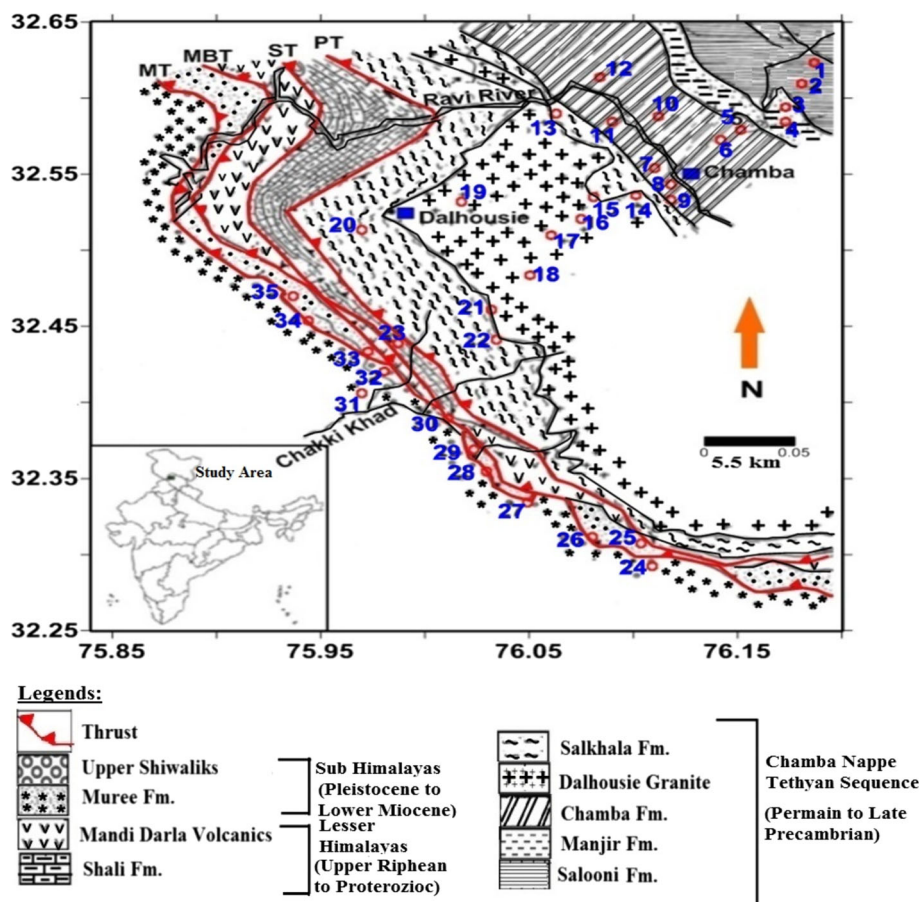


**Experimental techniques**

RAD7 produced by Durrige Company, USA, has been used for monitoring radon activity concentration in soil gas. For soil gas sampling, a hollow steel probe of 3 cm diameter and 130 cm length with disposable sharp awl that can make steel probe favorable for drilling into the soil and prevent soil from blocking the probe was used. This steel probe is placed into the ground at a depth of about 0.8–1.0 m by pounding using a hammer and drive in head. A thin solid bullet (punching wire) is used to displace the tip and allows the lower end of the probe to be in contact with the soil surface at the required depth. A hand pump pumping through a specially designed rubber tube (with two filters, one for the moisture and one for dust) was connected with hollow steel to collect gas into sample bag. If the flux is strong enough, then the hand pump can be replaced by an alpha pump (an automatic pump having pumping rate 1 l/min) to collect soil gas in the evacuated sample bags having capacity of 3 l (Walia et al. 2005). Before collecting the soil gas in sample bags, the tube and the probe must be flushed for air, which might be present, by pumping it for approximately 1 min.

Sample bags used for collecting soil gas are Tedlar standard sample bags (manufactured by SKC Inc. company), which utilize a lightweight, patented compact two fittings of inert polypropylene that combine the hose/valve and the septum holder which allow the sample bag to be used in a closed circuit for radon analysis. With the increase in the humidity detection efficiency of RAD7 decreases, therefore before making the measurement RAD7 must be dry. To achieve this, it is purged for sometime using drying unit and RAD7 humidity reading has been inspected to make it sure that relative humidity readings during the measurement period are below 10 %. The soil samples were immediately analyzed with RAD7 at the site after the collections without any delay; therefore, decay correction is neglected. For many instruments, radon and thoron interfere with each other. Generally, it is difficult to measure one isotope accurately in the presence of the other. But compared to other instruments, the RAD7 is much less susceptible to radon thoron interference due to its ability to distinguish the isotopes by their unique alpha particle energies. The RAD7 separates radon and thoron signals and counts the two isotopes at the same time with little interference from one to the other. In order to measure

**Fig. 2** Geological map of Chamba region along with the measurement points and tectonic features (MBT = Main Boundary Thrust; PT = Panjal Thrust; ST = Shali Thrust and MT = Muree Thrust) (modified after Thakur 1998)



radium activity concentration in soil, surface soil samples were collected from undisturbed sites at each location. Samples were dried in an oven at about 100 °C for 1–2 h to remove the moisture content and then crushed to pass through a 150- $\mu$ m-mesh sieve to homogenize it. Then, a sample of 300 g was weighed, and finally, a split of the prepared sample was packed in a standard plastic container; after properly tightening the threatened lid, the containers were sealed with adhesive tape and left for at least 4 weeks ( $>7$  half-lives of  $^{222}\text{Rn}$  and  $^{224}\text{Ra}$ ) before counting by gamma spectrometry in order to ensure that the daughter products of  $^{226}\text{Ra}$  achieve equilibrium with their respective parent radionuclide's. The samples were analyzed by using high-resolution gamma spectrometry system consists of coaxial  $n$ -type high-purity germanium (HPGe) detector having 50 % relative efficiency with respect to 7.62 cm  $\times$  7.62 cm NaI (TI), and its energy resolution measured in terms of the full width at half maximum (FWHM) is 2.1 keV at 1,332.5 keV of  $^{60}\text{Co}$  gamma energy at 25 cm from the top of the detector. Spectrum stabilized 8 K MCA (PHAST, Electronics Division, BARC) along with other electronic accessories was coupled with the HPGe detector. Details of the measurement technique are given elsewhere (Chinnaesakki et al. 2011).

## Results and discussion

With an aim to understand tectonic and geological controls on soil gas radon variations in the study regions, detailed surveys were conducted in a continuous stretch of 2 weeks during the month of April 2010, to ascertain the spatial variation of soil gas under stable meteorological conditions. Thirty-seven soil gas samples were collected in the Dharamshala region (Fig. 1), and thirty-five samples were collected in the Chamba region (Fig. 2). Along with soil gas radon samples, thirty-four surface soil samples were also collected from both Dharamshala and Chamba region. Spatial distribution of soil gas sampling is important, but it is not always possible to choose the limits of sampling interval and have dense sampling due to the following: tough terrain, proper site location, no/poor soil gas flux, and other practical/field problems which are difficult to avoid. In the present study, we also faced these problems, and even though we hammered down the probe at many locations but failed to get enough gas emission, to have the samples as rocks in this area are devoid of any primary porosity due to underlying hard rock formations. For these reasons, we have to satisfy ourself with the confined number of samples we were able to collect during field works.

**Fig. 3** Soil gas radon activity concentrations along with error bars in Dharamshala region

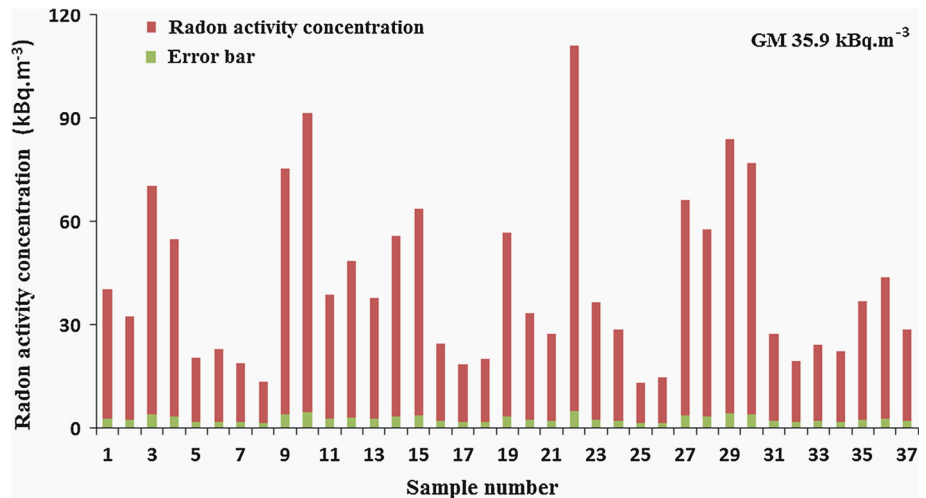


**Fig. 4** Soil gas radon activity concentrations along with error bars in Chamba region

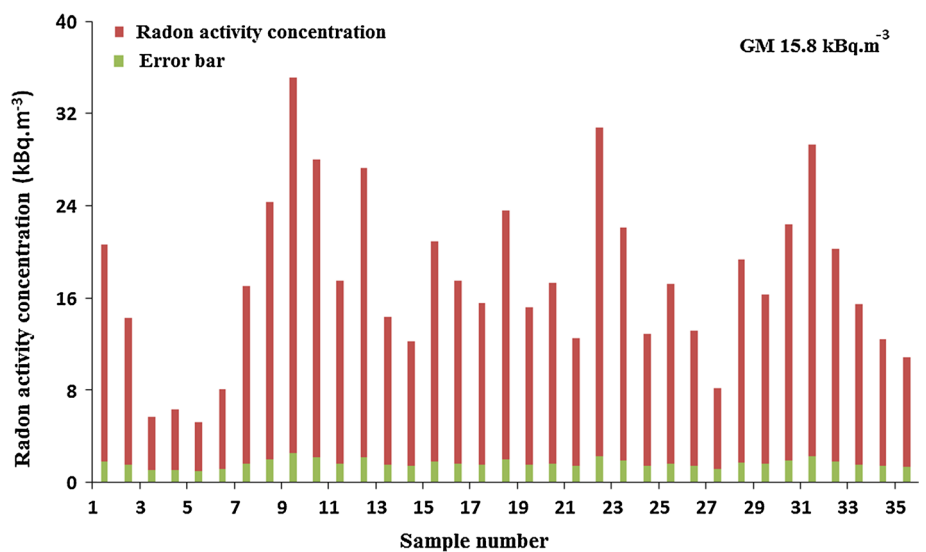


**Table 1** Average soil gas radon concentrations in different geological formations of Dharamshala region

S. no.	Geological formation	No. of sample	G.M. of radon concentration (kBq m <sup>-3</sup> )	Maximum (kBq m <sup>-3</sup> )	Minimum (kBq m <sup>-3</sup> )	Geometrical SD
1	Shivaliks	7	31.6	70.2 ± 3.9	13.6 ± 1.5	1.7
2	Dharamshala sandstone	14	27.9	66.2 ± 3.8	13.2 ± 1.5	1.6
3	Alluvium	12	45.5	110.8 ± 5.0	18.8 ± 1.7	1.7
4	Dharamkot	2	35.4	43.6 ± 2.9	28.7 ± 2.2	1.2
5	Dharamshala trap	2	80.2	83.7 ± 4.3	76.8 ± 4.1	1.0

The results of soil gas radon activity concentration measurements along with error bars (shown by green color) are shown by bar graphs in Figs 3 and 4, for Dharamshala and Chamba regions, respectively. The soil gas radon variation with minimum, maximum, and geometrical mean (G.M.) of soil gas radon activity concentration in different geological formations of Dharamshala and Chamba regions has been tabulated in Tables 1 and 2, respectively. Average

radium activity concentrations observed in different geological formations of Dharamshala and Chamba regions have been tabulated in Tables 3 and 4.

In Dharamshala region, the soil gas radon activity concentrations have been observed to be varying from 13.2 ± 1.5 to 110.8 ± 5.0 kBq m<sup>-3</sup>, with a geometrical mean of 35.9 kBq m<sup>-3</sup> and geometrical standard deviation of 1.8. The radon activity concentration in soil gas of the

**Table 2** Average soil gas radon concentrations in different geological formations of Chamba region

S. no.	Geological formation	No. of sample	G.M. of radon concentration (kBq m <sup>-3</sup> )	Maximum (kBq m <sup>-3</sup> )	Minimum (kBq m <sup>-3</sup> )	Geometrical SD
1	Chamba formation	8	17.4	35.6 ± 2.5	5.2 ± 1.0	1.5
2	Salooni	2	17.2	20.6 ± 1.8	14.3 ± 1.5	1.2
3	Manjir	2	6.0	6.3 ± 1.1	5.7 ± 1.1	1.1
4	Salkhala	3	16.1	12.2 ± 1.4	30.8 ± 2.3	1.5
5	Granite	7	18.3	23.6 ± 2.0	15.2 ± 1.6	1.2
6	Shiwalik	4	15.8	29.3 ± 2.2	8.2 ± 1.2	1.6
7	Muree	9	15.0	19.3 ± 1.8	10.9 ± 1.3	1.2

**Table 3** <sup>226</sup>Ra activity in different geological formations of Dharamshala region

S. no.	Geological formation	<sup>226</sup> Ra activity (Bq kg <sup>-1</sup> )
1	Dharamshala trap	45.4 ± 1.7
2	Shiwalik	36.9 ± 1.6
3	Alluvium	38.3 ± 1.4
4	Dharamkot limestone	40.4 ± 1.9
5	Dharamshala sandstone	43.9 ± 1.7

Average <sup>226</sup>Ra activity in soil samples of Dharamshala: 40.4 ± 1.7 Bq kg<sup>-1</sup>

**Table 4** <sup>226</sup>Ra activity in different geological formations of Chamba region

S. no.	Geological formation	<sup>226</sup> Ra activity (Bq kg <sup>-1</sup> )
1	Chamba formation	44.4 ± 1.7
2	Salooni	39.6 ± 1.6
3	Manjir	33.9 ± 1.4
4	Granite	40.9 ± 1.7
5	Shiwalik	33.6 ± 1.8
6	Muree	39.1 ± 2.1

Average <sup>226</sup>Ra activity in soil samples of Chamba: 38.6 ± 1.7 Bq kg<sup>-1</sup>

Dharamshala area is higher than the radon activity concentration in soil gas of non-tectonic of Ropar district of Punjab by Singh et al. (2009) (11.6–27.4 kBq m<sup>-3</sup>) but are comparable than those reported for soil gas in nearby neotectonic areas of Himachal Pradesh by Singh et al. (2006) (1.1–82.2 kBq m<sup>-3</sup>). Average radium activity concentration in the soil samples collected from different geological formations of Dharamshala region is found to be 40.4 ± 1.7 Bq kg<sup>-1</sup>.

Average radium activity concentration in soil samples collected from Dharamshala formation is found to be 45.4 ± 1.8 Bq kg<sup>-1</sup>. Fourteen samples of soil gas have been collected and analyzed to find the radon activity concentration in soil gas of Dharamshala formation. The geometrical mean and geometrical standard deviation in

soil gas radon activity concentration in Dharamshala formation has been found to be 27.9 kBq m<sup>-3</sup> and 1.6, respectively. Average radium activity concentration in soil samples of Shiwalik formation of Dharamshala region is 36.9 ± 1.6 Bq kg<sup>-1</sup>. The geometrical mean and geometrical standard deviation of radon activity concentration in Shiwalik formation has been found to be 31.6 kBq m<sup>-3</sup> and 1.7, respectively. Twelve samples of soil gas have been collected and analyzed from the alluvium formation of Dharamshala region. Soil gas radon activity concentration in this formation varies between 18.8 ± 1.7 and 110.8 ± 5.0 kBq m<sup>-3</sup>, with a geometrical standard deviation of 1.7. Geometrical mean of soil gas radon activity concentration in alluvium formation is found to be 45.5 kBq m<sup>-3</sup>. Soil gas radon activity concentration and radium activity concentration in soil samples collected from Dharamkot limestone formation (Fig. 1) of the study zone have been found to have an average value of 35.4 kBq m<sup>-3</sup> and 40.4 ± 1.9 Bq kg<sup>-1</sup>, respectively, while average activity concentration of radium (45.4 ± 1.7 Bq kg<sup>-1</sup>) and soil gas radon activity concentration in soil samples collected from Dharamshala traps is 45.4 ± 1.7 Bq kg<sup>-1</sup> and 80.2 kBq m<sup>-3</sup>, respectively.

In Dharamshala region, soil gas radon activity concentration in Dharamshala and Shiwalik formation is comparatively smaller than other geological formations of this region irrespective of the higher radium content in the soil samples of Dharamshala formation. This may be due to compact packing of the sandstones resulting in poor conditions for migration of radon gas from some deep seated source of radon. Soil gas radon activity concentration in alluvium formation has been found to be comparatively higher than the sandstones of Dharamshala and Shiwalik formations. This may be due to the comparatively higher porosity of soil as compared to Shiwalik/Dharamshala group which are having compact basement that hinder the radon migration. Soil gas samples collected from the locations near Manjhi Khad (MJK) (sample no 19 and 27, Fig. 1) show comparatively higher radon activity concentration of 56.6 ± 3.4 and 66.2 ± 3.8 kBq m<sup>-3</sup>, respectively. Comparatively higher values of radon activity

concentration near Manjhi Khad may be due to the influence of transverse lineaments on the migration of radon gas. It has been observed that soil gas samples collected from the Dharamshala traps (viz. 29 and 30) (Fig. 1) have comparatively much higher radon activity concentration of the order of  $80.2 \text{ kBq m}^{-3}$ . The limestone succession of Dharamkot formation and Dharamshala traps is sandwiched between two steeply inclined thrusts which may be the reason for better migration of radon to the surface.

To better understand the whole scenario of soil gas radon variation in Dharamshala across the tectonic features such as MBT, MBT-2, and MCT, efforts were made to undertake transverse profiles (Fig. 5a, b, c) across the existing fault zones in Dharamshala region. It has been

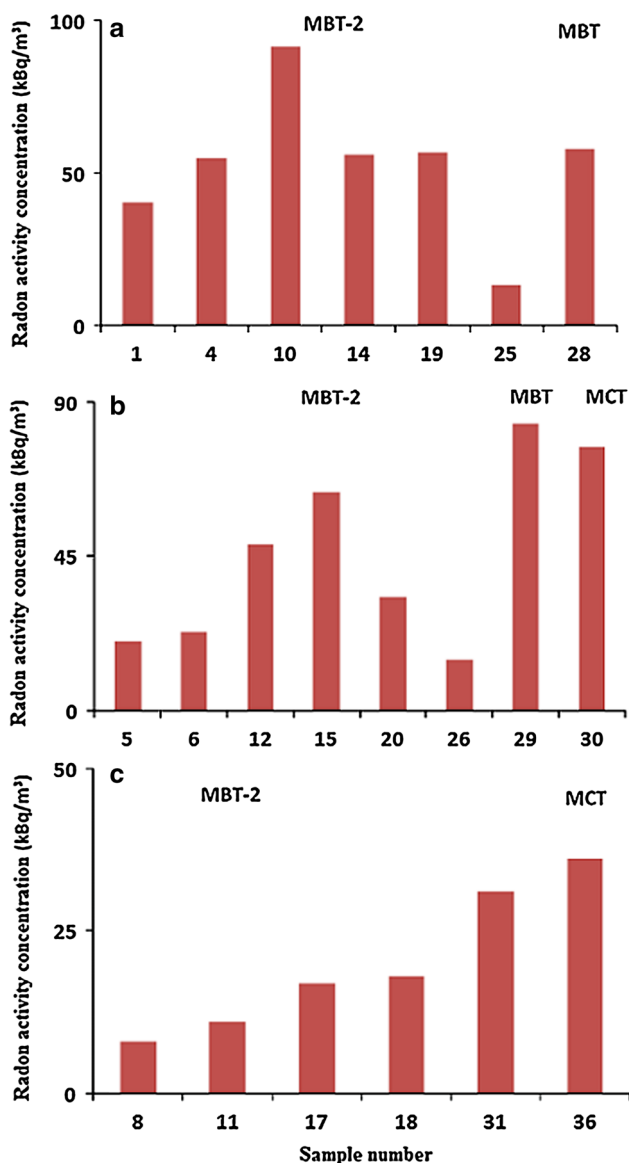


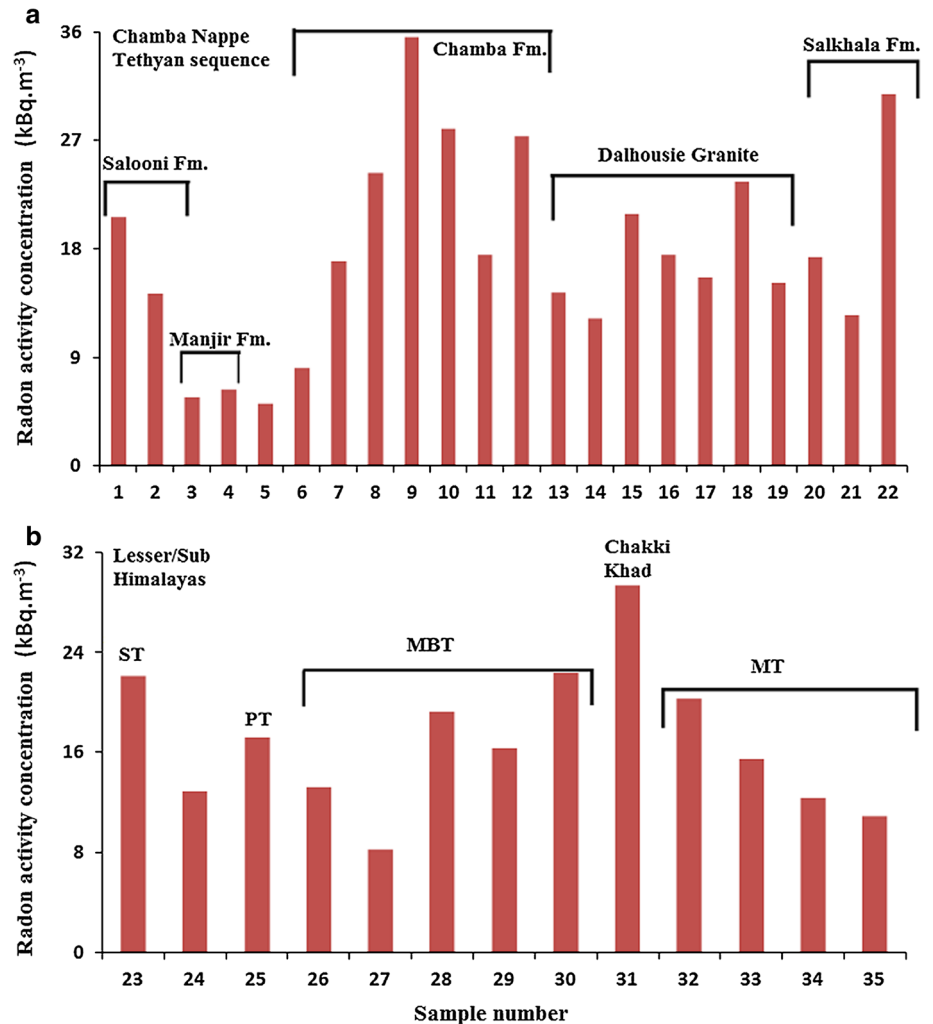
**Fig. 5** a Soil gas radon variation across MBT in Dharamshala region. b Soil gas radon variation across MCT in Dharamshala region. c Soil gas radon variation across MBT-2 in Dharamshala region

observed that the radon activity concentration shows a very wide range of variation, and peaks of concentration were obtained near the MBT, MBT-2, and MCT. Similar type of profiling has already been done previously by a Walia et al. (2008) across MBT-2 for fault delineation study. Soil gas radon activity concentration is found to be comparatively higher near the tectonic structures in both surveys, but unlike to the results obtained previously in 2008, there was no rapid increase in radon activity concentration in soil near the fault. Soil gas radon activity concentration has been found to be higher in the alluvium formation in the both the surveys, and results reveal that few sampling points have more or less similar trend for radon activity concentration variation. Differences in the soil gas radon activity concentrations observed in these two surveys may be due to the possible seasonal effects/change in meteorological conditions prevailing during these surveys or may be due to the fact that sampling points are not exactly the same. Moreover, soil gas radon activity concentration as well as the soil gas permeability varies not only from one survey to another, but also among different measurement points/locations within each survey (Chen et al. 2008).

Radon activity concentration in the thirty-five soil gas samples collected from the Chamba region of Himachal Pradesh (Fig. 2) has been found to be varying from  $5.2 \pm 1.0$  to  $35.6 \pm 2.5 \text{ kBq m}^{-3}$  with geometrical mean of  $15.8 \text{ kBq m}^{-3}$  and geometrical standard deviation of 1.6. The radon activity concentration in soil gas of the chamba area is slightly higher than the radon activity concentration in soil gas of Ropar district of Punjab by Singh et al. (2009) ( $11.6\text{--}27.4 \text{ kBq m}^{-3}$ ), but are lower than those reported for soil gas in neotectonic area near Dharamshala region of Himachal Pradesh by Singh et al. (2006) ( $1.1\text{--}82.2 \text{ kBq m}^{-3}$ ). Average radium activity concentration in soil samples collected from Chamba region has been found to be  $38.6 \pm 1.7 \text{ Bq kg}^{-1}$ .

Eight samples of soil gas have been collected and analyzed from the Chamba formation (Fig. 6a). Soil gas radon activity concentration in this formation varies between  $5.2 \pm 1.0$  and  $35.6 \pm 2.5 \text{ kBq m}^{-3}$  with a geometrical standard deviation of 1.5. Average radium activity concentration and geometrical mean of radon activity concentration in the soil samples of Chamba formation are found to be  $44.4 \pm 1.7 \text{ Bq kg}^{-1}$  and  $17.4 \text{ kBq m}^{-3}$ , respectively. Geometrical mean of soil gas radon activity concentration in Salkhala formation is found to be  $16.1 \text{ kBq m}^{-3}$ , and geometrical standard deviation is 1.5. In Chamba region, thirteen soil gas samples were also collected on/near the MBT, ST, PT, and MT (sample no 23–35) (Fig. 6b). Geometrical mean of soil gas radon activity concentration in these samples has been found to be  $16 \text{ kBq m}^{-3}$ , with geometrical standard deviation of 1.4.

**Fig. 6** **a** Soil gas radon variation across Chamba nape tethyan sequence in Chamba region. **b** Soil gas radon variation across ST, PT, MBT and MT in Chamba region



In Chamba region, average soil gas radon activity concentration in the Dalhousie granites and Salooni formation is found to be comparatively higher than Manjir formation (Fig. 6a). This can be attributed to the higher activity of  $^{226}\text{Ra}$  in soil samples of Salooni ( $39.6 \pm 1.6 \text{ Bq kg}^{-1}$ ) and granite formations ( $40.9 \pm 1.7 \text{ Bq kg}^{-1}$ ) as compared to Manjir formation ( $33.9 \pm 1.4 \text{ Bq kg}^{-1}$ ) (Table 4). Comparatively, higher values of soil gas radon activity concentration (sample nos 8, 9, 10, and 12) in Chamba formation (Fig. 6a) may be related to a present neotectonic active fault along the Ravi River (Joshi 2004) or may be due to the comparatively higher radium activity concentration in the soil samples of Chamba formation. This active fault initially recognized on morphotectonic criteria gained significance as a seismogenic structure following the 1995 earthquake. An attempt will be made in the future studies to delineate this neotectonic fault using soil gas technique.

Salkhala formation in the Chamba region consists of phyllite, quartzitic phyllite, micaceous quartzites, and

occasional bands of gray marbles and volcanic layers together with biotite and garnet-biotite schists near the granitic bodies. G.M. of soil gas radon activity concentration in Salkhala formation is found to be  $16.1 \text{ kBq m}^{-3}$ , and geometrical standard deviation is 1.5. Average soil gas radon activity concentration in the Dalhousie granites and Salooni formation is found to be comparatively higher than Manjir formation (Fig. 6a). This can be attributed to the higher activity of radium in soil samples of Salooni ( $39.6 \pm 1.6 \text{ Bq kg}^{-1}$ ) and granite formations ( $40.9 \pm 1.7 \text{ Bq kg}^{-1}$ ) as compared to Manjir formation ( $33.9 \pm 1.4 \text{ Bq kg}^{-1}$ ). It has been observed that the Shiwalik formation in Chamba region (along the MT) yields comparatively less average soil gas radon activity concentration (G.M.  $15.8 \text{ kBq m}^{-3}$ ), as compared to Shiwalik formation (G.M.  $31.6 \text{ kBq m}^{-3}$ ) of Dharamshala region. Comparatively, higher soil radon activity concentration in Dharamshala region may be due the presence of local transverse lineaments in the region. Comparatively, less radon activity concentration in the soil gas samples



collected from Muree formation may be due to the compact packing of sandstones in this formation, resulting into poor migration of radon gas, thus corroborating the results obtained by Walia et al. (2008) in the sandstones of Dharamshala region.

Efforts were made to undertake transverse profiles across the fault zones and have dense sampling in Chamba region, but the tough geological/geographical conditions made it impossible to do the task efficiently and in planned way. Most part of the area is underlain by hard rock formation ranging in age from Paleozoic to Triassic. These older rocks are devoid of any primary porosity. Thirteen soil gas samples were collected and analyzed on/near the Main Boundry thrust, ST, PT and MT (sample no 23–35) (Fig. 6b). Comparatively, higher values of soil gas radon activity concentration (sample nos 23, 32, and 31) in Chamba region (Fig. 6b) may be related to a present neotectonic active fault along the Ravi River (Joshi 2004).

The results obtained by different studies showed that the soil gas radon activity concentration may vary over a wide range depending on weather conditions, climatic factors, and soil type (Chernik et al. 2001; Durrani and Ilic 1997). The observed values of radium activity concentration in soil samples in the present study are less than the recommended action level  $370 \text{ Bq kg}^{-1}$  (OECD 1979) but slightly higher than the worldwide average value of  $35 \text{ Bq kg}^{-1}$  for the same radionuclide in soils reported by UNSCEAR (2000).

Linear regression model equations to represent the soil gas radon activity concentration and radium activity concentration data of Dharamshala and Chamba have been observed (Figs. 7, 8). It has also been observed that soil gas radon activity concentration in Chamba region has a positive correlation of 0.55 with the observed radium activity concentration in the soil samples collected from different locations near the sampling points of soil gas

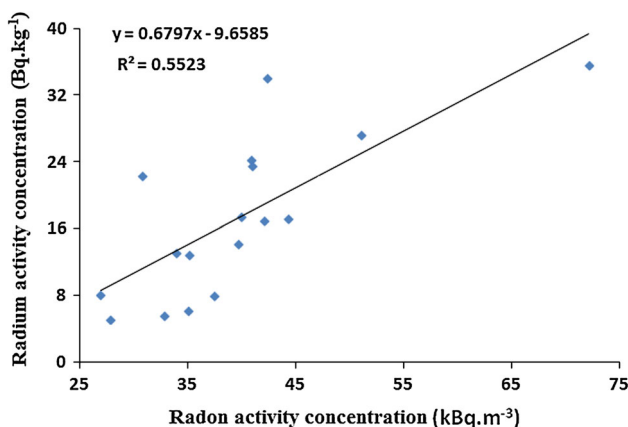


Fig. 7 Correlations between radon and radium activity concentration in Chamba region

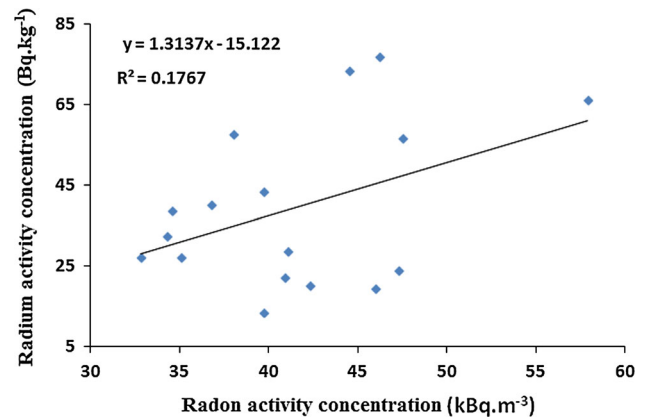


Fig. 8 Correlations between radon and radium activity concentration in Dharamshala region

(Fig. 7), while comparatively weak positive correlation of 0.18 has been observed between soil gas radon activity concentration and radium activity concentration in Dharamshala region (Fig. 8). From the present study, it seems in the Chamba region radon is not only controlled by radium but also influenced by tectonic activity and geological setting of the area, whereas in the Dharamshala region radon is mostly controlled by tectonic setting of the area.

### Conclusion

Results of radon activity concentration in soil gas and radium activity concentration in soil samples of Dharamshala and Chamba regions of NW Himalayas are reported here. The study area was selected after literature surveys about the geology and tectonic of the areas. Soil gas radon activity concentration has shown large variation in both Dharamshala and Chamba regions, while radium activity concentration in soil samples is more or less same in both the regions. The observed values of radium activity concentration in soil samples in the present study are less than the recommended action level but slightly higher than the worldwide average value. Radon and radium have shown poor correlation in Dharamshala region as compared to Chamba region with the overall poor correlation coefficient of 0.20. It is observed from the radon anomalies pattern in the studied regions that anomalies are not distributed on the conspicuous faults locations only. It is reported that soil gas radon emission not only depend upon radium activity concentration but also on other factor viz. tectonic activity, geology of the area, soil porosity, etc. From the poor correlation of radium activity concentration and radon activity concentration in the present study, it can be concluded that the radon activity concentration may be mainly controlled by tectonic and geological features

present in the area. Further, the anomalous radon concentration activity has also been observed along the local drainage patterns and river pathways suggesting the presence of some neotectonic feature which is also reported in some other studies.

**Acknowledgments** The authors are thankful to National Science Council of Taiwan and Department of Science and Technology for supporting this work financially under the project (NSC 100-2116-M-492 -002).

## References

- Baubron JC, Rigo A, Toutain J (2002) Soil–gas profile as a tool to characterize active tectonic areas: the Jault Pass example (Pyrenees, France). *Earth Planet Sci Lett* 196:69–81
- Bolinder AS, Owen DE, Schumann RR (1993) A preliminary evaluation of environmental factors influencing day-to day and sessional soil-gas radon concentrations. In: Gunderson LCS, Wanty RB (eds) *Field studies of radon in rocks, soil, and environment*, USGS. C. K. Smoley Publishers, pp 23–31
- Chen J, Falcomer RLJ, Weirsdima J, Beryman L (2008) Long term monitoring of soil gas radon and permeability at two reference sites. *Radiat Prot Dosim* 131:503–508
- Chernik DA, Titov VK, Lashkov AB, Amosov DA (2001) Substantiation of the radon concentration in the soil air in estimating the radon risk of territories. *ANRI* 4:29–33 (in Russian)
- Chinnaesakki S, Chopra M, Kumar S, Arora V, Sartandel SJ, Bara SV, Tripathi RM, Puranik VD, Bajwa BS (2011) Assessment of natural radioactivity in soil samples and comparison of direct and indirect measurement of environmental air kerma rate. *J Radioanal Nucl Chem*. doi:10.1007/s10967-011-1192-x
- Choubey VM, Bist KS, Saini NK, Ramola RC (1999) Relation between soil–gas radon variation and the different lithotectonic units of Garhwal Himalaya, India. *J Appl Radiat Isot* 51(5):587–592
- Choubey VM, Bartarya SK, Ramola RC (2000) Radon in Himalayan springs: a Geohydrological control. *Environ Geol* 39(6): 523–530
- Choubey VM, Bartarya SK, Saini NK, Ramola RC (2001) Impact of geohydrology and neotectonic activity on radon concentration in groundwater of intermontane Doon Valley, Outer Himalaya, India. *Environ Geol* 40(3):257–266
- Choubey VM, Bartarya SK, Ramola RC (2005) Radon variations in an active landslide zone along Pindar River in Chamoli District, Garhwal Lesser Himalaya, India. *Environ Geol* 47(6):745–750
- Ciotoli G, Guerra M, Lombardi S, Vittori E (1998) Soil radon survey for tracing seismogenic faults: a case study in the Fucino basin, Central Italy. *J Geophys Res* 103(B10):781–794
- Ciotoli G, Etiopie G, Guerra M, Lombardi S (1999) The detection of concealed faults in the Ofanto Basin using the correlation between soil–gas fracture surveys. *Tectonophysics* 301:321–332
- Ciotoli G, Lombardi S, Annunziatellis A (2007) Geostatistical analysis of soil–gas data in a high seismic Intermontane basin: the Fucino plain, Central Italy. *J Geophys Res* 112:B05407. doi:10.1029/2005JB004044
- Cox ME (1983) Summit outgassing as indicated by radon, mercury and PH mapping, Kilauea volcano, Hawaii. *J Volcanol Geotherm Res* 16:131–151
- Crenshaw WB, Williams SN, Stoiber RE (1982) Fault location by radon and mercury detection at an active volcano in Nicaragua. *Nature* 300:345–346
- Durrani SA, Ilic R (1997) *Radon measurements by etched track detectors: applications in radiation protection, earth sciences, and the environment*. World Scientific, Singapore
- Etiopie G, Lombardi S (1995) Evidence for radon transport by carrier gas through faulted clays in Italy. *J Radioanal Nucl Chem* 193:291–300
- Fu CC, Yang TF, Walia V, Cheng CH (2005) Reconnaissance of soil gas composition over the buried fault and fracture zone in southern Taiwan. *Geochem J* 39:427–439
- Gansser A (1964) *Geology of the Himalayas*. Wiley, New York
- Gundersen LCS, Reimer GM, Agard S (1988) The correlation between geology, radon in soil gas, and indoor radon in the reading prong. In: Marikos M (ed) *Proceedings of the GEORAD conference: geological causes of radionuclide anomalies*, Missouri Department of Natural Resources Special Publication 4, pp 91–102
- Joshi DD (2004) A seismogenic active fault in the western Himalaya. *Curr Sci* 87:7–10
- King CY, King BS, Evans WC, Zhang W (1996) Spatial radon anomalies on active faults in California. *Appl Geochem* 11:497–510
- Kothiyari GC, Pant PD, Joshi M, Luirei K, Malik JN (2010) Active faulting and deformation of quaternary Landform Sub-Himalaya, India. *Geochronometria* 37:63–71
- Kumar A, Singh S, Mahajan S, Bajwa BS, Kalia R, Dhar S (2009) Earthquake precursory studies in Kangra valley of North West Himalayas, India, with special emphasis on radon emission. *Appl Radiat Isot* 67:1904–1911
- Kumar A, Walia V, Singh S, Bajwa BS, Mahajan S, Dhar S, Yang TF (2012) Earthquake precursory studies at Amritsar Punjab, India using radon measurement techniques. *Int J Phys Sci* 7(42):5669–5677
- Kumar A, Walia V, Yang TF, Hsien CH, Lin SJ, Eappen KP, Arora BR (2013) Radon-thoron monitoring in Tatun volcanic areas of northern Taiwan using LR-115 alpha track detector technique: pre calibration and installation. *Acta Geophys* 61(4):958–976
- Mahajan AK, Viridi NS (2000) Preparation of landslides hazard zonation map of Dharamsala Town and adjoining areas, District Kangra (H.P.). Project report, H.P. Government. p 45
- Mahajan AK, Kumar S, Chabak SK (1997) Local gravity anomaly and geotectonics in the Dharamsala and Palampur area, North West Himalayas. *J Geol Soc India* 50:75–84
- OECD (1979) Organization for economic cooperation and development. Report by a group of Experts of the OECD, Nuclear Energy Agency, OECD, Paris
- Papastefanou C, Manolopoulou M, Stoulos S, Ioannidou A, Gerasopoulos E (2001) Radon measurements along active faults in the Langadas basin, northern Greece. *Nat Hazards Earth Syst Sci* 1:159–164
- Schumann RR, Owen DE (1988) Relationship between geology, equivalent uranium concentration, and radon in soil gas, Fairfax County, Virginia: USGS open file report 88–18, p 28
- Singh S, Sharma DK, Dhar S, Randhawa SS (2006) Geological significance of soil gas radon: a case study of Nurpur area district Kangra Himachal Pradesh India. *Radiat Meas* 41(4):482–485
- Singh J, Singh H, Sing S, Bajwa BS (2009) Measurement of soil gas radon and its correlation with indoor radon around some areas of Upper Siwaliks. *J Radiol Prot* 29:1–9
- Tanner AB (1964) Radon migration in the ground: a review. In: Adams JAS, Lowder WM (eds) *The natural radiation environment*. University of Chicago Press, Chicago, pp 161–190
- Thakur VC (1998) Structure of the Chamba nappe and position of the Main Central Thrust in Kashmir Himalaya. *J Asian Earth Sci* 16(2–3):269–282
- UNSCEAR (2000) Report of the United Nations scientific committee on the effects of atomic radiation: sources and effects of ionizing radiation, vol 1. United Nations, New York

- Vaupotic J, Gregoric A, Kobal I, Zvab P, Kozak K, Mazur J, Kochowska E, Grzadziel D (2010) Radon concentration in soil gas and radon exhalation rate at the Ravne Fault in NW Slovenia. *Nat Hazards Earth Syst Sci* 10:895–899
- Wadia DN (1957) *Geology of India*, 3rd edn. McMillan and Co., London
- Walia V, Su TC, Fu CC, Yang TF (2005) Spatial variations of radon and helium concentrations in soil–gas across the Shan-Chiao fault, Northern Taiwan. *Radiat Meas* 40(2–6):513–516
- Walia V, Virk HS, Bajwa BS (2006) Radon precursory signals for some earthquakes of magnitude >5 occurred in N-W Himalaya. *Pure Appl Geophys* 163:711–721
- Walia V, Mahajan S, Kumar A, Singh S, Bajwa BS, Dhar S, Yang TF (2008) Fault delineation study using soil–gas method in Dharamsala area, NW Himalayas, India. *Radiat Meas* 43:S337–S342
- Walia V, Yang TF, Hong WL, Lin SJ, Fu CC, Wen KL, Chen CH (2009a) Geochemical variation of soil–gas composition for fault trace and earthquake precursory studies along the Hsincheng Fault in NW Taiwan. *Appl Radiat Isot* 67:1855–1863
- Walia V, Lin SJ, Hong WL, Fu CC, Yang TF, Wen KL, Chen CH (2009b) Continuous temporal soil–gas composition variations for earthquake precursory studies along Hsincheng and Hsinhua faults in Taiwan. *Radiat Meas* 44:934–939
- Walia V, Yang TF, Lin SJ, Kumar A, Fu C, Chiu JM, Chang HH, Wen KL, Cheng CH (2013) Temporal variation of soil gas compositions for earthquake surveillance in Taiwan. *Radiat Meas* 50:154–159
- Williams SN (1985) Soil radon and elemental mercury distribution and relation to magmatic resurgence at long valley caldera. *Science* 229:551–553